International Journal of Multiphase Flow 37 (2011) 84–97

Contents lists available at ScienceDirect

International Journal of Multiphase Flow

journal homepage: www.elsevier.com/locate/ijmulflow

Two-phase refrigerant flow instability analysis and active control in transient electronics cooling systems

TieJun Zhang [a,*], John T. Wen [a,b], Yoav Peles [a], Juan Catano [a], Rongliang Zhou [b], Michael K. Jensen [a]

[a] Center for Automation Technologies and Systems, Department of Mechanical, Aerospace & Nuclear Engineering, Rensselaer Polytechnic Institute, 110 8th Street, Troy, NY 12180, USA
[b] Department of Electrical, Computer & System Engineering, Rensselaer Polytechnic Institute, 110 8th Street, Troy, NY 12180, USA

ARTICLE INFO

Article history:
Received 16 April 2010
Received in revised form 25 June 2010
Accepted 26 July 2010
Available online 21 August 2010

Keywords:
Electronics cooling
Flow instability
Pressure-drop oscillation
Refrigeration system
Two-phase cooling
Active control
Transient heat load

ABSTRACT

Two-loop refrigeration systems are being explored for two-phase cooling of ultra high power electronic components. For effective and efficient thermal management of electronic systems, active control methods are desired to suppress inherent flow instabilities especially in transient applications. This paper presents a framework for the transient analysis and active control of pressure-drop flow instabilities under varying imposed heat loads. The external effects on boiling flow characteristics and the boiling oscillatory flow responses to transient heat load changes are studied. Flow instability margins can be quantitatively predicted from an analytical two-phase flow model. In addition, the effects of wall thermal inertia on flow oscillations is systematically investigated. Based on the theoretical analysis of oscillatory flow boiling of refrigerants, a set of active control schemes are developed and studied to suppress flow oscillations and to increase the critical heat flux. With the available control devices – inlet valve and supply pump – different active control schemes are studied to improve the transient two-phase cooling performance.

1. Introduction

Rapidly increasing power density of electronics is bringing critical thermal management problems (Garimella et al., 2008) in practical high-power electronics applications. The peak heat dissipation rate of next-generation electronic systems, such as radar, directed-energy lasers, and electromagnetic weapons, will exceed 1000 W/cm^2 in the near future (Kandlikar and Bapat, 2007; Lee and Mudawar, 2009). In fact, the surface temperature of most silicon-based electronics (e.g., widely used insulated-gate bipolar transistors) has to be maintained below 85 °C for safe operation. Meanwhile, in practical applications, large transient heat loads are imposed and needed to be efficiently and effectively dissipated. Conventional cooling solutions are inadequate for dynamic thermal managements of compact electronic systems. Two-phase cooling technology can provide effective schemes to address some of the high-heat-flux electronics cooling challenges (Lee and Mudawar, 2009; Webb et al., 2007; Schmidt and Notohardjono, 2002; Trutassanawin et al., 2006; Wadell et al., 2007; Beitelmal and Patel, 2006; Kandlikar et al., 2006; Thome, 2006), since the latent heat of vaporization can be utilized.

To ensure higher heat removal efficiency and larger safe transient operation margin, low-temperature refrigeration systems are being explored for two-phase cooling of ultra high power electronic components. Conventional vapor compression cycles, or so-called direct refrigeration cooling, offer a solution for dynamic thermal management of electronic systems (Lee and Mudawar, 2009; Schmidt and Notohardjono, 2002; Trutassanawin et al., 2006; Wadell et al., 2007; Beitelmal and Patel, 2006; Catano et al., 2010). However, their cooling capability would be limited by the critical heat flux (CHF) condition, which would require the exit mass quality to be lower than one (Lee and Mudawar, 2009). Two-loop indirect refrigeration cooling systems, as a promising alternative of conventional refrigeration cycles, have many successful applications ranging from spacecrafts and underwater vehicles (Wang et al., 2010; Gilmore, 2002) to emerging electronics cooling (Lee and Mudawar, 2009; Chang et al., 2006; Zhou et al., 2009; Zhang et al., 2009). Due to the inherent subcooled boiling advantage, two-loop cooling systems have been demonstrated to be far more effective at dissipating high-power heat fluxes. Such systems can provide the flexibility of choosing different working fluids and pressure levels in the primary and secondary loops, and also offer the scalability for the removal of multiple distributed heat loads with a centralized chiller.

Two-phase cooling systems with high subcooled boiling are not problem free since they are prone to various flow boiling instabilities. For example, flow boiling oscillations may modify the hydrodynamics of the flow, introduce severe structural vibrations, generate acoustic noise, and can jeopardize the structural integrity of the system. But, most importantly, flow oscillations can lead to

* Corresponding author. Tel.: +1 518 276 2125; fax: +1 518 276 4897.
E-mail addresses: zhangt6@rpi.edu, tjzhang@ieee.org (T.J. Zhang).

0301-9322/$ - see front matter © 2010 Elsevier Ltd. All rights reserved.
doi:10.1016/j.ijmultiphaseflow.2010.07.003

premature initiation of the CHF condition. On the other hand, most of the existing studies focus on removing the heat at the device level, while active cooling at the system level has not received much attention especially for transient applications. Recently, these critical operational issues have been recognized and recommended in (Garimella et al., 2008) for future research: New "concepts for dampening or elimination of potential two-phase loop flow instabilities, and concepts for two-phase loop feedback flow control" are needed in active and transient thermal management of next generation military, automotive, and harsh-environment electronic systems.

Knowledge about flow instabilities is of particular importance for better design, control, and performance prediction of any two-phase system, especially the design of large/fast transient electronics cooling systems (Garimella et al., 2008; Lee and Mudawar, 2009; Kandlikar et al., 2006; Thome, 2006; Bergles et al., 2003). If there is no compressible volume upstream of a boiling system, the Ledinegg instability may occur when the flow system operates in the two-phase negative-slope region (Zhang et al., 2009; Kakac and Bon, 2008; Yin, 2004; Xu et al., 2005). Inappropriate supply pressure drop will trigger a sudden flow excursion to either a subcooled or a superheated operating conditions. As noted by Bergles et al. (2003), pressure-drop oscillations, a prevalent dynamic flow instabilities, occur in systems when two conditions are satisfied: there must be a compressible volume upstream of the boiling channel, and the channel pressure drop must decrease with increasing mass flowrate in the negative-slope flow region. A compressible volume of gas may exist in long boiling channels ($L/D \geqslant \sim 150$) or can be artificially introduced by placing a surge tank upstream of the heated section (Kakac and Bon, 2008; Yin, 2004). Considering the dynamic interactions between a compressible volume and the heated channels, the mass flowrate, pressure drop, and wall temperatures oscillate with a long period and large amplitude. Appreciable research efforts have been focused on the modeling and analysis of dynamic flow instabilities (Kakac and Bon, 2008; Lee and Yao, 2010; Ozawa et al., 1979; Liu et al., 1995; Kakac and Cao, 2009). In Liu et al. (1995), an empirical fourth-order polynomial was obtained to fit the experimental steady-state characteristics under a fixed heat load, and a dynamical analysis of pressure-drop oscillations with a planar model was performed. Based on the planar model, the existence, the uniqueness, and the stability of the limit-cycle of pressure-drop oscillations was theoretically proven, and the complete bifurcation diagram of the dynamic system was provided (Liu et al., 1995).

Two questions still remain to be answered; How does a transient imposed heat load affect dynamic flow boiling instabilities and cooling capabilities? And, what should be the active control strategy to suppress flow instabilities under transient heat loads? Limited results have been reported in the open literature about dynamic instability analysis and active control in transient refrigeration cooling systems, except for passive control methods with inlet restrictors (Kuo and Peles, 2009) and the inlet microheater-driven seed bubble flow stabilizing method (Xu et al., 2009). These static instability suppression methods are at the cost of much larger pumping power since additional pressure drop arises due to the restrictors. Active two-phase flow control may provide an alternative to suppress the refrigerant flow instability. Most recently, in Zhang et al. (2010), we developed a set of dynamic modeling, theoretical analysis, and model-based active control approaches for pressure-drop flow oscillations in boiling microchannel systems. However, this earlier effort is limited to fixed heat load and working fluid – water, which is not desirable for electronics cooling applications. In addition, thermal aspects were not addressed in that study (Zhang et al., 2010). However, in large-scale cooling applications, evaporator wall thermal inertia does have significant effects on transient flow conditions.

In the two-loop refrigeration system, flow boiling instability is one of the biggest operation problems for effective and efficient dynamic thermal management of electronics. This paper provides additional physical insight about two-phase thermal-fluid dynamics and proposes new concepts for model-based active flow instability analysis and control in transient electronics cooling systems under critical heat flux constraints. Advanced flow instability control strategies are based on dynamic thermal-fluid models. For boiling microchannel systems, no dynamic thermal-fluid model is widely accepted for transient and active thermal management study. Therefore, in this paper, we use conventional-scale two-phase flow models to evaluate general analysis and control methodologies, which could be extended to microchannel thermal-fluid systems.

2. System description

A typical two-loop electronics cooling system configuration (Lee and Mudawar, 2009; Webb et al., 2007; Zhang et al., 2009) is schematically shown as in Fig. 1. In the primary loop, a highly subcooled flow is directed to the heat sink (evaporator); compared to saturated boiling, subcooled boiling elevates the critical heat flux significantly, which is advantageous for high heat flux cooling. A secondary vapor compression cycle is used to dissipate heat to the ambient by using a fluid-to-fluid heat exchanger. Moreover, with the two-loop structure, distributed multiple heat loads could be handled with simple and small pump loops, all of which could be coupled to a centralized chiller (secondary vapor compression cycle, VCC). The coupled vapor compression cycle enables the two-loop cooling system to remove heat from the cold side to the hot side – a feature that is desirable in high heat flux cooling in harsh environments and not shared by the single loop pumped cooling systems (Chang et al., 2006; Zhou et al., 2009). The inclusion of the vapor compression cycle in the two - loop system also elevates the temperature difference between the refrigerant and the ambient cooling media, resulting in increased system cooling capacity.

The surge tank in Fig. 1 represent the inherent compressibility of primary two-phase cooling loop. This upstream compressible volume interacts with two-phase boiling flow inside the heat sink; thus, pressure-drop refrigerant flow oscillations may occur, which will deteriorate the cooling performance significantly and cause burn out of the electronic devices. Detailed flow pattern description and analysis will be given in the consequent sections. Notice that the cooling capability of the fluid-to-fluid heat exchanger is assumed to be sufficiently large, and, as a result, dynamic interaction between the secondary VCC loop and primary pumped loop can be ignored.

Since non-dielectric coolants are not preferred for electronics cooling, wide-temperature-range dielectric fluids, such as the common refrigerant R-134a, is a good choice as the primary coolant. In this study, the main component parameters are taken from our experimental testbed at Rensselaer Polytechnic Institute (Catano et al., 2010), where cartridge heaters are used to represent the uniform heat load generated from electronics. These heaters immersed in the refrigerant (R-134a) emulate the evaporators in a two-phase electronics cooling system.

3. Preliminaries

3.1. Two-phase flow principles

3.1.1. Basic balance equations

To quantify flow boiling instabilities in uniformly heated channels, a one-dimensional momentum balance is applied to two-phase flow in a horizontal channel:

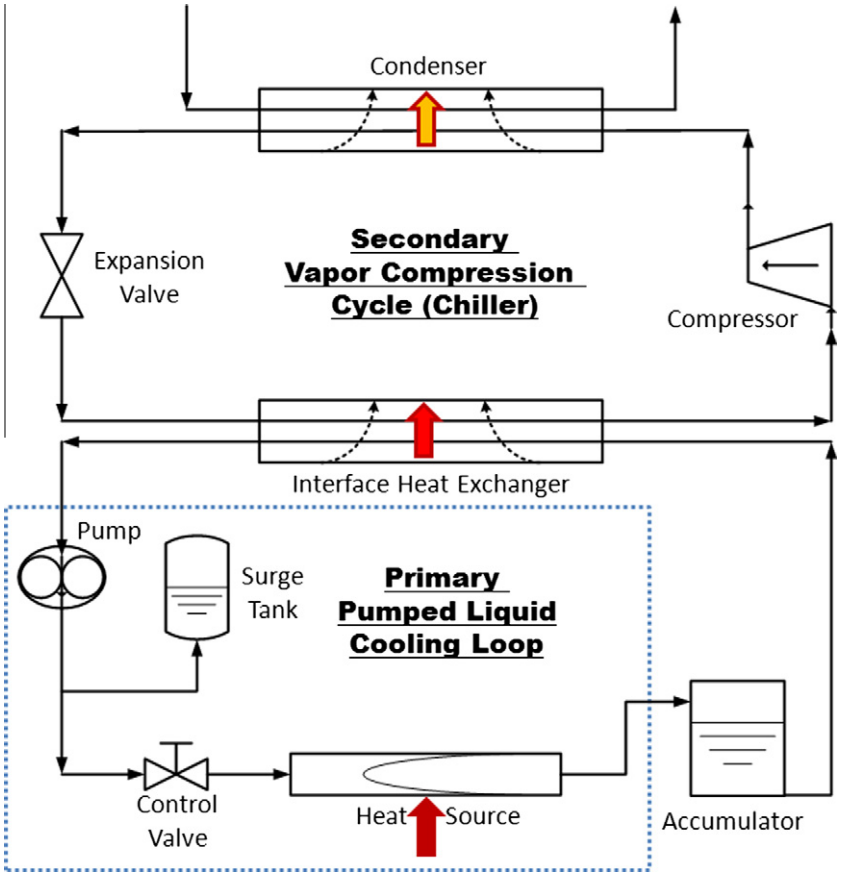

Fig. 1. Schematic of two-loop electronics cooling system.

$$\frac{\partial \dot{m}}{\partial t}+\frac{\partial}{\partial z}\left(\frac{\dot{m}^2}{\rho A}\right)+\frac{\partial (PA)}{\partial z}+F_{visc}=0 \tag{1}$$

where $\dot{m}$ is the mass flowrate, $\dot{m}=\rho A\upsilon=\rho\dot{V},A$ is the cross-sectional area, ρ is the fluid density, and F_{visc} is the frictional shear force. Integrating from $z=0$ to L, one obtains the lumped momentum balance equation:

$$\begin{aligned}&\frac{dG}{dt}=\frac{1}{L}(\Delta P_S-\Delta P_D)\\&G=\frac{\dot{m}}{A},\quad \Delta P_S=P_{in}-P_e,\quad \Delta P_D=\Delta P_a+\Delta P_f\end{aligned} \tag{2}$$

where G is the mass flux, ΔP_S is the supply pressure drop, the demand pressure drop ΔP_D includes all the accelerational and frictional pressure drops and other potential inlet/exit pressure losses, P_{in}/P_e are the inlet/exit pressures, respectively.

In addition, one-dimensional mass and energy balances can be used to characterize the fluid mass and heat transport in a heated channel,

$$\frac{\partial(\rho A)}{\partial t}+\frac{\partial \dot{m}}{\partial z}=0 \tag{3}$$

$$\frac{\partial(\rho A u)}{\partial t}+\frac{\partial(\dot{m}h)}{\partial z}=\frac{q}{L} \tag{4}$$

where u is the specific internal energy, h the specific enthalpy, and q the imposed heat input. At steady state, the mass flow rate is kept constant along the channel, and the energy balance equation (4) under the uniform heat load becomes

$$\frac{\partial h}{\partial z}=\frac{q}{\dot{m}\cdot L}=\frac{q''\cdot S}{G\cdot A\cdot L} \tag{5}$$

where S is the surface area. From Eq. (5), it can be inferred that for uniform heat flux q'', the local enthalpy changes linearly with the axial distance from the inlet; accordingly, the mass quality in the boiling channel is nearly piecewise linear at steady state, as used in power generation based boilers (Astrom and Bell, 2000).

3.1.2. Flow characteristics

To better understand the flow instability in boiling channels, consider the channel pressure-drop demand curve as a function of mass flowrate for constant heat flux (Fig. 2). When the flow rate is sufficiently large, the flow is single-phase liquid (the right region of the curve). As the mass flowrate is continuously reduced while all other conditions are unchanged, boiling will commence at some pressure drop. Further reduction in the mass flux will gradually cause vigorous boiling. Since frictional and accelerational pressure drops tend to increase as the void fraction (and mass quality) increases, a point can be reached in which the pressure-drop slope reaches a minimum. This point is frequently termed the onset of flow instability (OFI) (Zhang et al., 2009; Xu et al., 2005; Lee and Yao, 2010). When the flow is close to the local minimum of flow characteristic curve, pure pressure-drop oscillatory behavior is usually exhibited; when the flow is close to the local maximum of the flow characteristics curve, pressure-drop oscillations superimposed with density-wave oscillations may occur (Kakac and Bon, 2008; Yin, 2004).

For a uniform imposed heat load along the channel, a piecewise linear profile is used to approximate the transient flow quality in the two-phase region (Astrom and Bell, 2000; Eborn, 2001). Based on this approximation, analytical flow characteristics of the heated channel can be derived according to (Eborn, 2001),

$$\Delta P_c=\frac{4L}{D}\frac{fG^2}{2\bar{\rho}}=\frac{2L}{D}\frac{fG_c^2}{\rho_l}\left[\left(\frac{G}{G_c}\right)^2\frac{\rho_l}{\bar{\rho}}\right]=\frac{2L}{D}\frac{fG_c^2}{\rho_l}g(x) \tag{6}$$

$$x=\frac{G}{G_c},\quad G_c=\frac{q}{A(h_v-h_{in})} \tag{7}$$

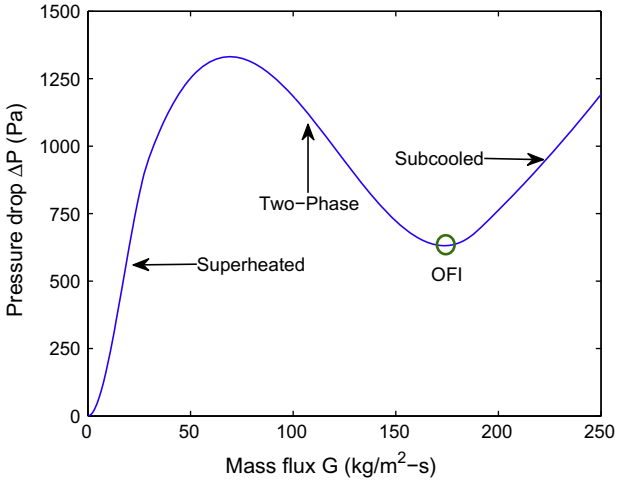

Fig. 2. Schematic two-phase flow characteristics of boiling channel.

where f is the liquid friction factor, G_c is the mass flux corresponding to complete evaporation (i.e., the exit flow is at quality of one) of inlet subcooled liquid with the heat load q, and the nonlinear function $g(x)$ under complete/partial/no boiling conditions is

$$g(x) = x^2\left(\frac{\rho_l}{\rho}\right) = \begin{cases} \left[a_1 + \frac{a_2(a_3+1)}{2} - a_3\right]x^3 + a_3x^2, & 0 \leqslant x < 1 \\ \frac{a_1^2(a_3-1)}{2a_2}x^3 + \left[1 - \frac{a_1(a_3-1)}{a_2}\right]x^2 + \frac{a_3-1}{2a_2}x, & 1 \leqslant x < \frac{1}{a_1} \\ x^2, & \frac{1}{a_1} \leqslant x \end{cases} \tag{8}$$

$$a_1 = \frac{h_l - h_{in}}{h_v - h_{in}}, \quad a_2 = \frac{h_v - h_l}{h_v - h_{in}}, \quad a_3 = \frac{\rho_l}{\rho_v} \tag{9}$$

The local maximum and minimum of the pressure drop–mass flux curve always occur in the two-phase boiling region, $1 \leqslant x < 1/a_1$ (Eborn, 2001). By differentiating the local function $g(x)$ within this region and setting the quadratic function to zero, there will be two separate extrema if

$$\frac{\rho_l}{\rho_v} = a_3 \geqslant 1 + (4 + 2\sqrt{3})\frac{a_2}{a_1} = 1 + (4 + 2\sqrt{3})\frac{h_v - h_l}{h_l - h_{in}} \tag{10}$$

It follows that if the liquid/vapor density ratio on the left hand side is larger than the enthalpy ratio on the right hand side, the boiling system will exhibit pressure-drop flow oscillations. In particular, the extrema will coincide and no oscillations will be observed if the equality in Eq. (10) holds.

3.2. Two-phase flow instabilities

3.2.1. Ledinegg excursion

As discussed by Kakac and Bon (2008) and Zhang et al. (2009), flow boiling in a channel is susceptible to a static Ledinegg instability (flow excursion) when the slope of the demand pressure drop–mass flow curve becomes algebraically smaller than the loop supply pressure drop–mass flow curve:

$$\frac{\partial(\Delta P_D)}{\partial \dot{m}} < \frac{\partial(\Delta P_S)}{\partial \dot{m}} \tag{11}$$

To maintain system stability, the pump supply curve should be considered. If the slope of the pump supply curve has a smaller negative value compared with the demand curve, the system is unstable. This occurs because the pump cannot counteract even a small perturbation in the mass flow from the two-phase equilibrium condition, and a spontaneous shift to a more stable superheated or subcooled flow condition occurs, which deteriorates the heat dissipating performance. Recent studies (Zhang et al., 2009) have shown that increasing system pressure and channel diameter, reducing parallel channel number and channel length, and including an inlet restrictor can enhance flow stability in microchannels.

3.2.2. Pressure-drop oscillation

The compressible flow system marked by the dotted line in Fig. 1 is schematically shown in Fig. 3, where the subcooled working fluid is supplied to both the compressible surge tank and the boiling channel (evaporator). The upstream compressibility arises from two sources: (i) the vessel before pump connected to the main branch through a bypass valve; and (ii) the inlet manifold of the boiling test section.

In the presence of the upstream surge tank, the flow in the boiling channel interacts with the surge tank. From mass balance, the inlet mass flowrate of the overall system becomes, $\dot{m}_{in} = \dot{m} + \dot{m}_s$, or equivalently, $G_{in} = G + G_s$, where $\dot{m} = GA$ is the mass flowrate into the heated channel measured by a flow meter, and $\dot{m}_s = G_sA$ is the flowrate into/out of the surge tank. In the tank, the gas is assumed to be inert and isothermal (Kakac and Bon, 2008); thus, the pressure P and the gas volume V are subject to the following relationship:

$$P \cdot V = P_0 \cdot V_0 = constant \tag{12}$$

Taking the time derivative of Eq. (12) yields

$$\frac{dP}{dt} \cdot V + P \cdot \frac{dV}{dt} = 0$$
$$\frac{dP}{dt} = -\frac{P}{V}\frac{dV}{dt} = -\frac{P^2}{P_0V_0}\frac{dV}{dt} \tag{13}$$

The compressible gas volume change in the surge tank is proportional to the upstream liquid inflow with a density ρ_l,

$$\dot{m}_s = -\rho_l\frac{dV}{dt} \quad \text{or} \quad \frac{dV}{dt} = -\frac{\dot{m}_s}{\rho_l}$$

By substituting dV/dt into Eq. (13), and with $\dot{m}_s = \dot{m}_{in} - \dot{m} = A(G_{in} - G)$, one obtains

$$\frac{dP}{dt} = \frac{P^2}{\rho_l P_0 V_0}\dot{m}_s = \frac{P^2 A}{\rho_l P_0 V_0}(G_{in} - G) \tag{14}$$

As mentioned before, the momentum balance equation for the downstream boiling channel is expressed as follows:

$$\frac{dG}{dt} = \frac{1}{L}(P - P_e - \Delta P_D) \tag{15}$$

where the exit pressure, P_e, is usually regarded to be constant due to the presence of the downstream condenser. Therefore, Eqs. (14) and (15) constitute the pressure-drop boiling flow oscillation model.

3.2.2.1. Critical heat flux. The critical heat flux (CHF) condition dictates the practical thermal limit in flow boiling systems. When this process occurs, a rapid transition from a high heat transfer coefficient condition to a low heat transfer coefficient condition takes place. In high flux removal applications, knowledge of the CHF condition is vital to prevent device burnout.

The Katto correlation (Katto, 1978) is a widely accepted correlation for CHF prediction in tubular channels and expressed as follows:

$$q''_{chf} = q''_{co}\left(1 + K\frac{h_l - h_{in}}{h_v - h_l}\right) \tag{16}$$

where q''_{co} is the saturated CHF under different operating conditions (Katto, 1978; Carey, 2008), K is the inlet subcooling parameter, h_{in} is

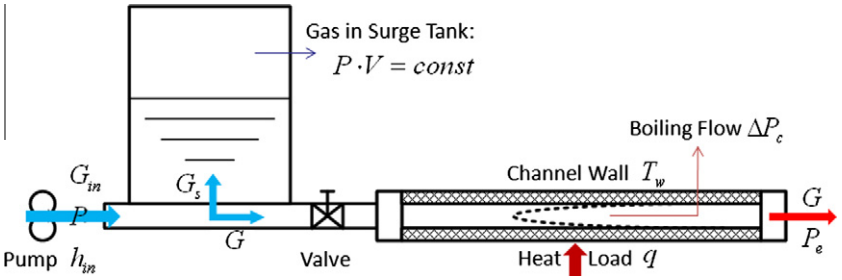

Fig. 3. Schematic of boiling channel with a upstream surge tank.

the inlet (subcooling) enthalpy, and h_l/h_v is the saturated liquid/vapor enthalpy. Katto's correlation shows that CHF increases with mass flow rate and inlet subcooling. To maintain safe operation of high power electronics, cooling systems must dissipate large imposed heat loads (which can change quite rapidly) effectively and quickly. Thus, it is important to study the critical heat flux condition especially in transient electronics cooling systems. This is unlike conventional fluid-to-fluid heat exchanger applications.

4. Dynamic flow instability analysis

To design dynamic thermal management systems for high power electronics, it is desirable to study the effects of multiple operating parameters on boiling associated flow oscillations.

4.1. Coolant and pressure effects

For complete fluid comparison, typical coolants such as deionized water, R-134a, and HFE-7100 are considered. Water has much higher thermal conductivity and latent heat of vaporization than typical refrigerants and coolants, such as R-134a and HFE-7100. However, water has much higher saturation temperature at atmosphere pressure. Therefore, for electronics cooling, sub-atmosphere system pressure is required to ensure a sufficiently low operating temperature.

As implied by the analytical flow characteristics and Eq. (10), larger liquid/vapor density ratios, ρ_l/ρ_v, result in more susceptibility to instabilities and larger flow oscillation amplitudes. As shown in Fig. 4, R-134a is less susceptible to flow instability at room temperature compared to HFE-7100 and water, and HFE-7100 becomes quite susceptible at lower temperatures (<0 °C). In general, water-based two-phase thermal management systems may have the most severe flow instability problems for a given operating temperature.

As for a given working fluid, it has been reported (Zhang et al., 2009; Kuo and Peles, 2009) that increasing the system pressure (i.e., a decreasing liquid-to-vapor density ratio) eventually will diminish flow instabilities. This is consistent with the analysis following Eq. (10) and Fig. 5, where the instability margin decreases with increasing system pressure for refrigerant R-134a. This, in turn, mitigates the possibility for the initiation of a premature critical heat flux condition induced by flow oscillations and significantly increases the corresponding maximum heat flux attainable of the system at elevated pressures (or low ρ_l/ρ_v).

4.2. Imposed heat load effects

To evaluate the effects of heat load on two-phase flow characteristics and flow oscillations, a cartridge heater immersed in an annular refrigerant channel serves as an evaporator, where the imposed heat load is uniformly distributed along the length of the heater. Notice that the operating conditions below are just for general methodology study.

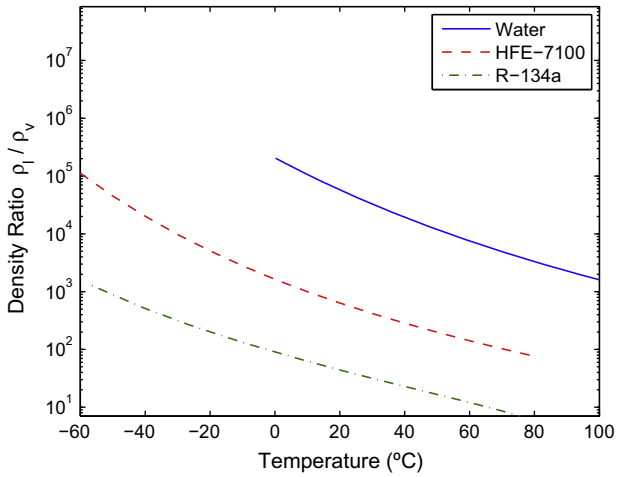

Fig. 4. Density ratio of different working fluids for electronics cooling.

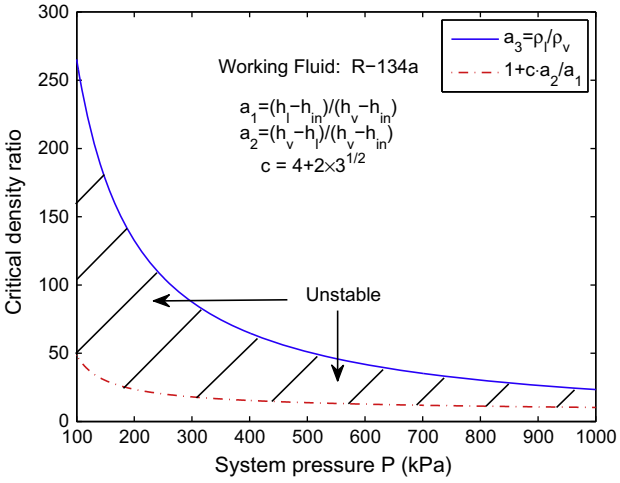

Fig. 5. Effect of system pressure on flow instabilities (solid: density ratio; dashed: enthalpy ratio).

Refrigerant R-134a is used in the subsequent quantitative simulation analysis, and the evaporator parameters are given by:

Heated channel length, $L = 0.4$ m.
Cartridge heater diameter, $D_c = 0.0127$ m.
Channel inner diameter, $D_i = 0.0206$ m.
Hydraulic diameter, $D = 0.0162$ m.
Cross-sectional area, $A = 2.0577 \times 10^{-4}$ m^2.

Heated surface area, $S = 0.0160\ m^2$.
Wall thermal inertia, $C_{pw}M_w = 2.304$ J/K.

At steady state, the following nominal operating conditions are chosen:

Inlet mass flowrate, $\dot{m}_{in} = 0.0144$ kg/s.
Inlet flow enthalpy, $h_{in} = 55.1486$ J/kg.
Exit flow pressure, $P_e = 2 \times 10^5$ Pa.
Initial system pressure, $P_0 = 2 \times 10^5$ Pa.
Compressible gas volume, $V_0 = 0.7 \times 10^{-3}\ m^3$.

4.2.1. Steady-state heat load effect

Based on the analytical two-phase flow model Eq. (6), the corresponding flow characteristics are shown in Fig. 6 for different imposed heat inputs ($q = 500, 1000, 1500, 2000$ W). As shown in Fig. 6, the two-phase region grows and the slope becomes more negative, when the imposed heating power increases. This, in turn, suggests that the heated flow system becomes more susceptible to flow boiling instabilities, and the flow oscillation amplitude magnifies with increasing heat load.

4.2.2. Transient heat load effect

Due to the presence of system compressibility, the flow inside the heated channel interacts with the upstream flow. When the boiling channel is filled with vapor, the flow is pushed into the upstream volume. Meanwhile, the inlet pressure continues to increase until it overcomes the channel demand pressure drop. Once this occurs, subcooled liquid rushes into the channel, and the imposed heat input evaporates the liquid until an additional cycle begins. Such behavior has been observed in multi-scale two-phase flow applications (Thome, 2006; Bergles et al., 2003; Kakac and Bon, 2008; Xu et al., 2005; Kuo and Peles, 2009; Zhang et al., 2010).

Practical electronic systems often operate in a dynamic mode rather than in a steady-state mode. Thus, it is important to study the effects of transient heat loads on boiling flow oscillations. In Fig. 7, a stepwise heat load changes are imposed on the channel. Within the first 10 s, self-sustained flow oscillations are observed from the transient flow G and system pressure P; the corresponding critical heat flux condition is calculated based on Eq. (16). It appears that the imposed power almost reaches the lower bound of the critical power ($q''_{chf} \times S$) at the minimum oscillatory flow condition. The imposed heat input is abruptly decreased from 1 kW to 0.5 kW after 10 s and then increased to 1.5 kW on the 40th second. In this case, the oscillations disappear, and the imposed heat flux is much lower than the CHF condition. This can be explained from the steady-state flow characteristics: the 0.5 kW heat input is not sufficient to boil the inlet flow (inlet mass flux $G_{in} = 70$ kg/m^2-s), and the exit flow is still at subcooled liquid conditions. Between the 40th second and the 70th second, a large heat input increase is imposed on the channel, the flow oscillates again with a large amplitude, and the imposed heat flux exceeds the critical heat flux, which will burn out the channel wall/electronics in practice; this is the damage that can not be tolerated in transient operation of cooling systems. When the heat load further increases to 2 kW, the flow oscillations diminish since superheated flow exits the heated channel. This means the heat transfer performance will decrease significantly, and the channel exit temperature will elevate greatly. This situation can also damage the electronics and thus should be avoided in electronics cooling applications. In addition, the corresponding phase portrait responses with different flow characteristics are shown in Fig. 8.

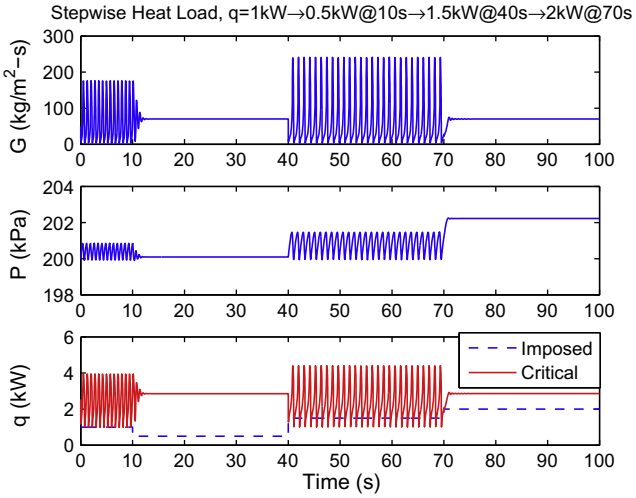

Fig. 7. Responses of boiling flow oscillation system to stepwise heat load changes ('critical': critical heat flux times surface area).

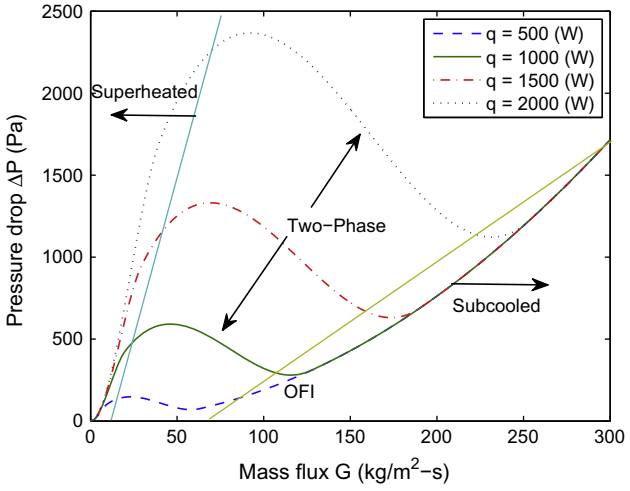

Fig. 6. Two-phase flow characteristics under different heat loads (dashed: 0.5 kW; solid: 1.0 kW; dashed-dot: 1.5 kW; dotted: 2.0 kW).

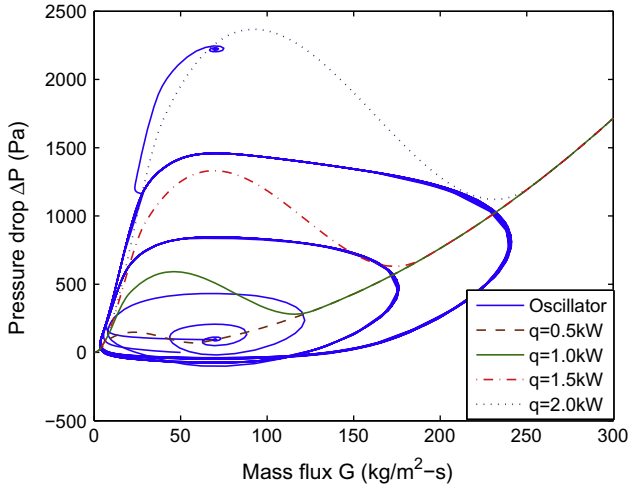

Fig. 8. Phase portrait of boiling flow oscillation system responses to stepwise heat load changes (dashed: 0.5 kW; solid: 1.0 kW; dashed-dot: 1.5 kW; dotted: 2.0 kW).

4.3. Wall thermal inertia effects

In many practical cases, the channel wall thermal inertia may significantly affect the system performance since it affects the amount of heat transferred into the refrigerant during a transient. With a wall energy balance, an extended lumped flow oscillation model can be obtained from Eqs. (14) and (15),

$$\frac{dP}{dt} = \frac{P^2 A}{\rho_l P_0 V_0}(G_{in} - G) \tag{17}$$

$$\frac{dG}{dt} = \frac{1}{L}(P - P_e - \Delta P_D) \tag{18}$$

$$\frac{dT_w}{dt} = \frac{q - q_r}{C_{pw} M_w}, \quad q_r = \alpha_r S(T_w - T_r) \tag{19}$$

where q_r is the actual heat transferred to the refrigerant (i.e., taking into account heat storage in wall), T_w is the wall temperature, and α_r the heat transfer coefficient of refrigerant. Then, the critical mass flowrate in (7) becomes,

$$G_c = \frac{q_r}{A(h_v - h_{in})}$$

This is consistent with our intuition that the actual heat input does affect the flow characteristics functions (6)–(8) in transient operation. In some extreme operating scenarios, for example, the critical heat flux condition will significantly change the flow regime inside the heated channel. Notice that simplified steady-state lumped-channel flow heat transfer and friction correlations are used here, $\alpha_r = 0.3Re_l^{0.8}Pr_l^{0.4}(k_l/D), f = 4Re_l^{-0.25}$. Note that the friction factor equation includes all channel inlet/exit losses and has been adjusted to match pressure drop characteristics of our experimental flow loop. The heat transfer coefficient expression, while quite simple, provides heat transfer coefficients comparable to those, for example, of Kandlikar (1990) over the range of conditions studied. The heat transfer coefficient is a lumped value for the entire length of the heated channel; because the oscillatory flow could cover a very wide range of operating conditions (transient, laminar, turbulent, nucleate dominated boiling, convection dominated evaporation, etc.), no single, simple correlation is available in the literature. The value of the estimated heat transfer coefficient does not affect the oscillatory flow characteristics but does affect only slightly the magnitude of the wall temperature oscillations.

In this study, the wall thermal inertia is the production of the wall heat capacity and mass, $\beta C_{pw} M_w = 2.304$ J/K, with a medium wall thermal inertia ratio $\beta = 1$. With the medium wall thermal inertia, the transient responses of flow oscillation system to periodic and stepwise heat loads are shown in Figs. 9 and 10, respectively. Fig. 11 depicts the transient responses for small wall thermal inertia, $\beta C_{pw} M_w$ with $\beta = 0.05$. In both Figs. 9 and 11, some imposed heat loads are lower than the CHF limits for oscillatory flow, whose trends are similar to the cases without inertia. Transient responses in the large wall thermal inertia case ($\beta = 5$) is shown in Fig. 12, where no oscillations occur.

To demonstrate the wall thermal inertia effects on flow oscillations more clearly, parametric trends are given in Fig. 13. The flow oscillation frequency is found to decrease with increasing wall inertia, and the oscillation amplitude increases then decreases with increasing wall inertia. Finally, no oscillation is observed with sufficiently large wall thermal inertia. In addition, the wall temperature oscillation amplitude decreases with increasing wall thermal inertia, which results in smaller thermal stresses. Flow boiling with very large wall thermal inertia can be characterized to be under constant wall temperature boundary condition, where the heat transfer coefficient is usually lower than that in constant heat flux cases. When the oscillatory flow temperature increases, the temperature difference between the wall and refrigerant becomes lower, then less heat is transferred from the wall to the refrigerant, therefore less vapor is generated, and flow oscillation is, accordingly, suppressed.

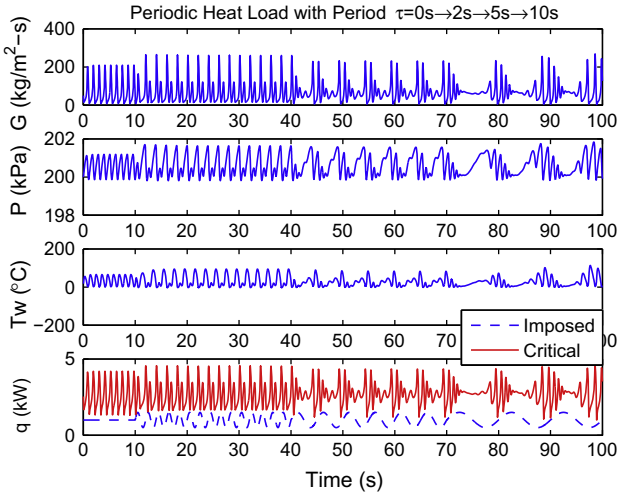

Fig. 9. Responses of boiling flow oscillation system with medium wall thermal inertia $\beta = 1$ to periodic heat load changes (dashed line: critical heat flux times surface area).

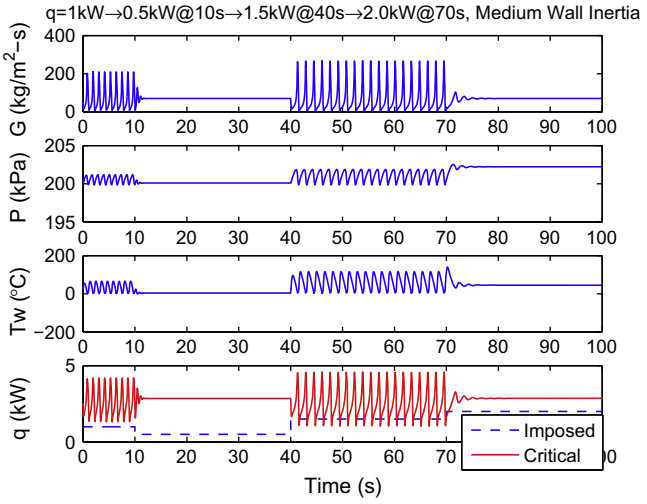

Fig. 10. Transient responses of boiling flow oscillation system with medium wall thermal inertia $\beta = 1$ (dashed line: critical heat flux times surface area).

5. Active flow instability control

In the above preliminaries, a two-state flow oscillation model (14) and (15) was developed to characterize the coupled hydrodynamics of the surge tank and boiling channel. Taking the derivative of (15) and substituting (14), assuming constant exit pressure ($P_e = constant$), the second-order compressible boiling flow model can be derived

$$\frac{d^2G}{dt^2} + \frac{1}{L}\frac{\partial(\Delta P_D)}{\partial G}\frac{dG}{dt} + \frac{P^2 A}{\rho_l P_0 V_0 L}G = \frac{P^2 A}{\rho_l P_0 V_0 L}G_{in} \tag{20}$$

where $G_{in} = \dot{m}_{in}/A$, P is measurable and its deviation is very small comparing with P_0. Note that the inlet mass flowrate, $\dot{m}_{in}$, is driven by a positive displacement supply pump, which can be used for active feedback control.

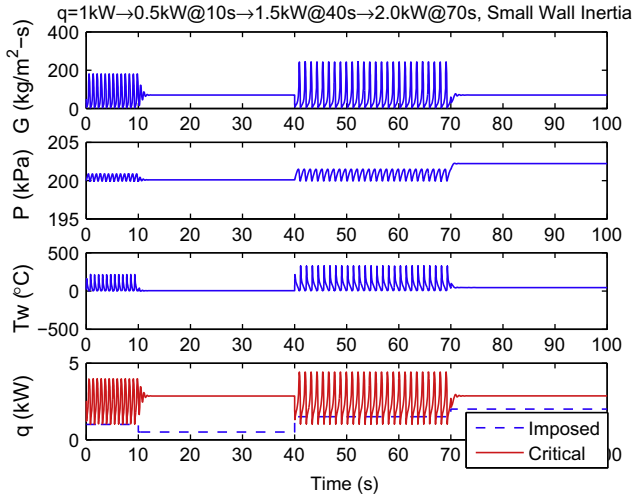

Fig. 11. Transient responses of boiling flow oscillation system with small wall thermal inertia $\beta = 0.05$ (dashed line: critical heat flux times surface area).

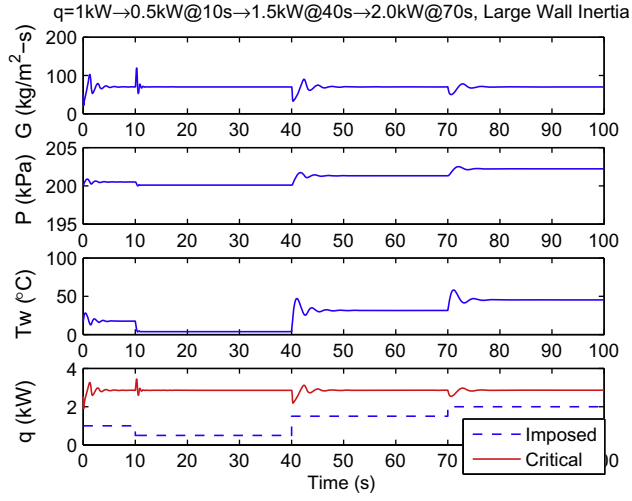

Fig. 12. Transient responses of boiling flow oscillation system with large wall thermal inertia $\beta = 5$ (dashed line: critical heat flux times surface area).

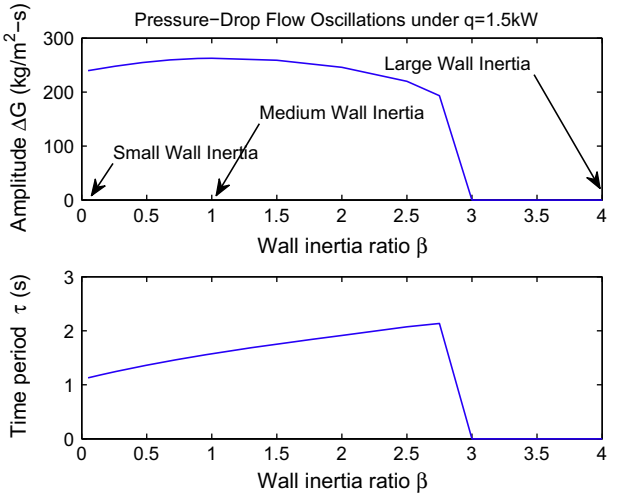

Fig. 13. Effect of wall thermal inertia on the flow oscillation amplitude and time period.

When the model (20) is considered, the most significant term for flow oscillations is the demand pressure-drop slope term, $\partial(\Delta P_D)/\partial G$, which is positive in the single-phase regions and, for the most part, negative in the two-phase boiling region. When the slope function is positive, the overall flow system is stable, otherwise, the flow system can be unstable. Similarities exists between this oscillatory behavior and Van der Pol oscillators, which are widely discussed in general nonlinear system and control theories (Khalil, 2002). It is, therefore, most probable that feedback control for the pressure-drop flow oscillation system can be developed.

For effective transient electronics cooling, the main control objectives are to maintain high transfer performance of two-phase flow inside the heated channel and to avoid pressure-drop flow oscillations even under large transient heat load changes. In order to develop active instability control methods, it is essential to analyze the stability of the compressible flow system (14) and (15) more explicitly as given in Appendix A.

Considering the compressible flow system in Fig. 3, two control elements are available for feedback: the inlet valve of the boiling channel and the supply pump in the system. Although inlet valve based control methods are widely accepted in practice, some theoretical analysis will be discussed here. In the pump-based flow control system, the manipulated variable – inlet flowrate, $\dot{m}_{in}$, – is linearly dependent on the positive displacement pump voltage. Thus, $\dot{m}_{in}$ is not fixed, and its change rate will affect the flow dynamics of both the surge tank and the boiling channel.

5.1. Inlet valve driven feedforward control

When there exists a control valve before the heated channel as in Fig. 3, this inlet valve can be used to suppress flow boiling oscillations. It should be noted that this scheme is subject to higher pressure loss and potential higher supply pumping power compared to a system without an inlet valve.

For the combined inlet valve and boiling channel system, the momentum balance is expressed according to

$$\frac{dG}{dt} = \frac{1}{L}(P - P_e - \Delta P_D) \tag{21}$$

$$\Delta P_D = \Delta P_c + \Delta P_r \tag{22}$$

where the overall pressure drop, ΔP_D, includes both the channel demand pressure drop ΔP_c in (6) and the inlet restrictor (valve) pressure drop ΔP_r,

$$\Delta P_r = \left(\frac{1}{C_r A_r}\right)^2 \frac{G^2}{\rho_l} = \kappa_r \cdot w_r \cdot \frac{G_c^2}{\rho_l} \cdot \left(\frac{G}{G_c}\right)^2 \tag{23}$$

where $\kappa_r = (A/C_r)^2 > 0$ is the valve characteristic coefficient, A_r the valve opening position within the range of $[0,1]$ and $w_r = 1/A_r^2$ in subsequent derivations. w_r increases with decreasing A_r from full opening position $A_r = 100\%$. Then the overall pressure drop is

$$\Delta P_D = \Delta P_c + \Delta P_r = \frac{G_c^2}{\rho_l}\left[\frac{2fL}{D} g(x) + \kappa_r w_r x^2\right] \tag{24}$$

By re-examining the oscillatory flow system (20), the pressure-drop flow instability is due to the existence of negative pressure-drop slope region of boiling channel. This implies that the characteristic slope of the combined valve/channel system will always remain positive if the control valve resistance can compensate for the negative slope portion of the channel flow characteristics. As for the combined channel/valve system, the overall pressure-drop slope can be derived from (22),

$$\frac{\partial(\Delta P_D)}{\partial G} = \frac{\partial(\Delta P_D)}{\partial x}\frac{\partial x}{\partial G} = \frac{G_c}{\rho_l}\left[\frac{2fL}{D} g'(x) + 2\kappa_r w_r x\right] \tag{25}$$

The aforementioned negative slope portion corresponds to the two-phase boiling region, that is, $1 \leqslant x \leqslant 1/a_1$. So the valve can be controlled such that the combined system pressure drop never decreases with increasing mass flux; that is, the overall pressure-drop slope is positive even in the two-phase region of boiling flow characteristics. The following flow stabilizing condition can then be defined

$$\kappa_c g'(x) + 2\kappa_r w_r x \geqslant 0, \quad \kappa_c = \frac{2fL}{D} \tag{26}$$

or equivalently

$$3(a_1x)^2 + 4(a_1x)\left[\frac{a_2}{a_1(a_3-1)} - 1\right] + 1\frac{\kappa_r w_r}{\kappa_c}\frac{4a_2}{a_1(a_3-1)}(a_1x) \geqslant 0 \tag{27}$$

Therefore, to maintain stable boiling flow, the following minimum valve (restrictor) pressure drop is required,

$$\Delta P_r = (\kappa_r w_r)\cdot\frac{G^2}{\rho_l} \geqslant \Delta P_r^m = -\frac{fLG_c^2}{D\rho_l}\frac{a_1(a_3-1)}{2a_2}\left[3a_1x + \frac{4a_2}{a_1(a_3-1)} - 4 + \frac{1}{a_1x}\right] \tag{28}$$

Furthermore, the above inequality (27) is always satisfied if

$$16\left[\frac{a_2}{a_1(a_3-1)} - 1 + \frac{\kappa_r w_r}{\kappa_c}\frac{a_2}{a_1(a_3-1)}\right]^2 - 12 \leqslant 0 \tag{29}$$

Thus, it can be concluded that the boiling flow in the combined valve and channel system is stable if the inlet valve pressure drop coefficient satisfies

$$\kappa_r w_r \geqslant \kappa_c\left[\left(1 - \frac{\sqrt{3}}{2}\right)\frac{a_1(a_3-1)}{a_2} - 1\right] \tag{30}$$

Notice that $a_1(a_3-1)/a_2$ represents the combined effect of inlet subcooling and density ratios, Fig. 14 shows that it has an upper bound (around 25) for a given working fluid under certain boundary conditions (inlet flowrate, inlet subcooling and fixed heat load). Accordingly, with the definition of $w_r = 1/A_r^2$, the flow stabilizing condition (30) becomes

$$A_r \leqslant \left[(24 - 12.5\sqrt{3})\frac{\kappa_c}{\kappa_r}\right]^{-1/2} \tag{31}$$

This means that in order to maintain stable flow boiling, the valve opening position must be lower than the value given in (31), which is independent of system pressure.

When the control valve position is sufficiently small, or equivalently, the inlet flow resistance is sufficiently large, the pressure drop of the combined valve and heated channel system will not decrease as the flowrate increases, like the dotted-dash curve in Fig. 15. This removes one of the triggering conditions for pressure-drop flow oscillations mentioned in Section 1. Thus, no flow oscillations will be observed for this case. In general, small valve opening position corresponds to much higher flow resistance and larger pressure loss, especially in the subcooled region, as observed in Fig. 15. So rather than a fixed inlet valve, it is more desirable to study active valve control strategies for the suppression of two-phase flow instabilities. The most straightforward method is to keep the valve fully-open for stable superheated or subcooled flow while reducing the valve opening position to the value predicted in the above analysis (31) during flow boiling. The reference curve for valve operation is like the dashed line in Fig. 15, which is a feedforward control scheme. The resulting transient control responses are shown in Fig. 16, where the oscillatory behavior of mass flux and pressure is eliminated with the valve controller (since the 10th second), even in the presence of stepwise heat load change after the 20th second. The corresponding phase portrait response curves are given in Fig. 17. It is evident that the controlled two-phase flow goes to the valve(restrictor)-imposed equilibrium under different heat loads. It should be noted that the valve actuator dynamics have not been included in this paper; rather instantaneous changes were assumed. However, valve response affects the settling time of the transient flow but does not affect the closed-loop two-phase flow system stability.

5.2. Inlet valve driven feedback control

As mentioned before, the introduction of a control valve is to ensure that the combined system pressure drop increases monotonically with mass flux, so no flow excursion or oscillation will take place. More specifically, the inlet valve pressure drop is used to compensate for the portion of the boiling flow pressure drop curve with a negative slope. A smaller inlet valve opening position generally leads to a higher pressure drop; thus, the overall pressure-drop slope becomes less negative, and the unstable flow range becomes more narrow. This trend can be used for feedback controller design. The transient oscillation amplitude is monitored in real time and regarded as an input signal for a proportional–integral (PI) valve controller. Eventually, the valve is gradually closed until no oscillation is detected.

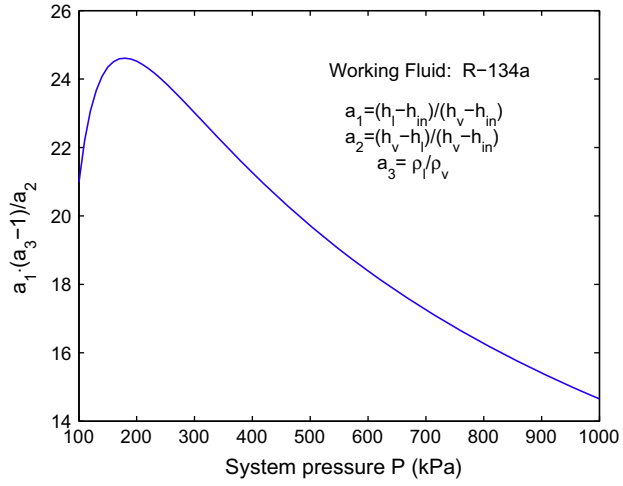

Fig. 14. Inlet subcooling ratio, $a_1/a_2 = (h_l - h_{in})/(h_v - h_l)$, vs. liquid/vapor density ratio, $a_3 = \rho_l/\rho_v$.

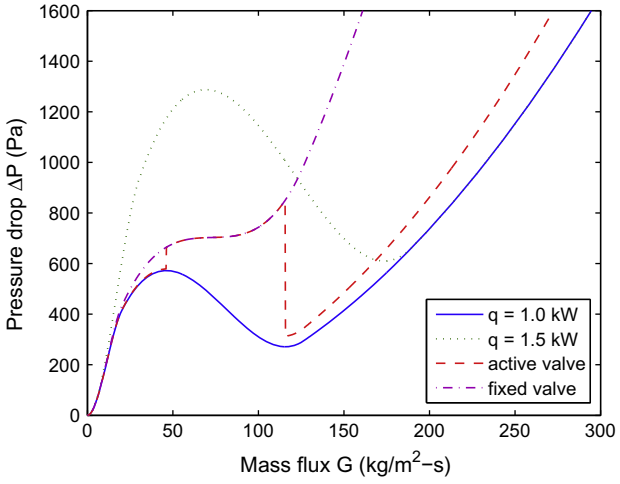

Fig. 15. Pressure drop–mass flux characteristics with active inlet valve feedforward control.

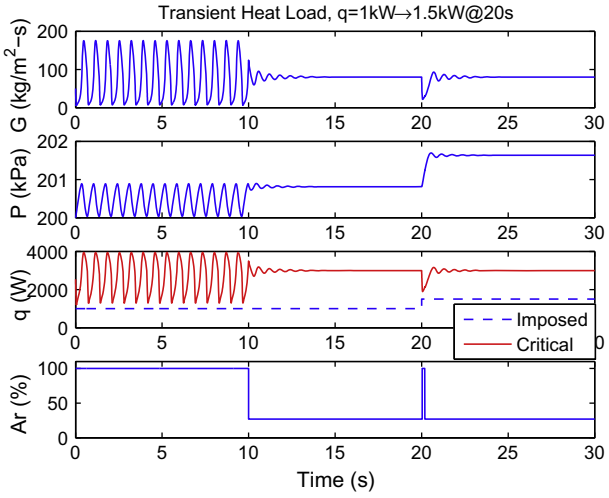

Fig. 16. Active feedforward control of pressure-drop flow oscillations driven by inlet valve (control implemented since the 10th second, heat load change from 1 kW to 1.5 kW since the 20th second).

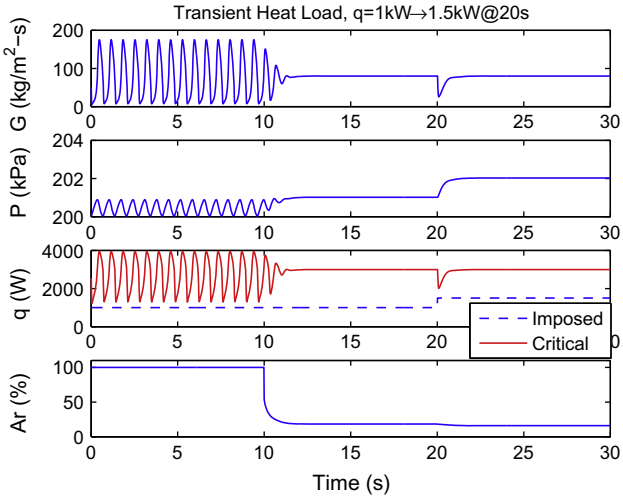

Fig. 18. Active feedback control of pressure-drop flow oscillations driven by inlet valve (control implemented since the 10th second, heat load change from 1 kW to 1.5 kW since the 20th second).

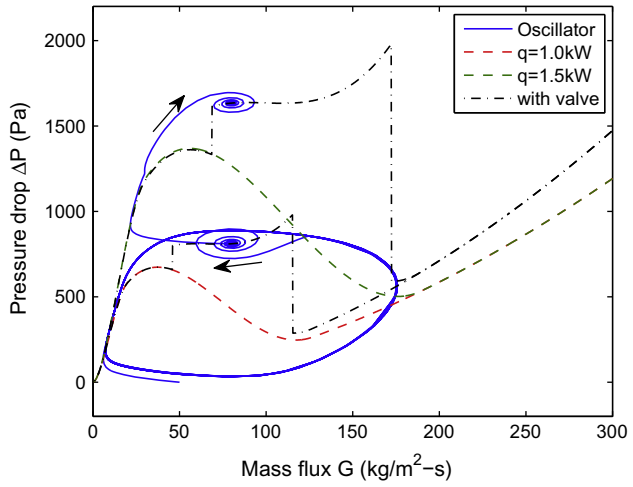

Fig. 17. Phase portrait of feedforward controlled flow oscillations driven by inlet valve (control implemented since the 10th second, heat load change from 1 kW to 1.5 kW since the 20th second).

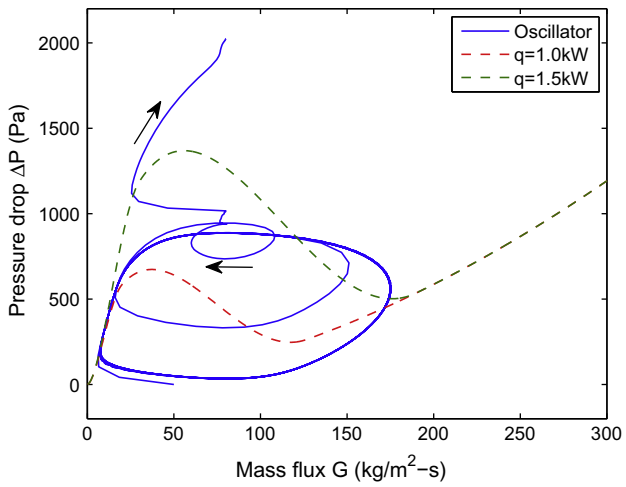

Fig. 19. Phase portrait of feedback controlled flow oscillations driven by inlet valve (control implemented since the 10th second, heat load change from 1 kW to 1.5 kW since the 20th second).

In this case study, a rolling one-second time window is set to detect transient flow deviation ($G_{max} - G_{min}$), where the sampling time is 0.02 s. A PI feedback controller, with proportional/integral gains $K_P = 1$, $K_I = 0.2$, is designed to manipulate the equivalent valve control variable, w_r, and hence, the actual valve opening position $A_r = 100 \times w_r^{-1/2}\%$. The corresponding closed-loop control results are given in Fig. 18 and the phase portrait in Fig. 19.

5.3. Supply pump driven feedback control

Although the inlet valve can suppress the upstream compressible flow instability, it suffers from high pressure loss and high supply pumping power. Alternatively, the inlet positive displacement pump can also be used to regulate the downstream flow conditions. In this case, the inlet restrictor (valve) can be removed so that no additional valve pressure loss is induced. It means that the overall demand pressure drop, ΔP_D, is the same as the channel pressure drop, ΔP_c, in (6).

5.3.1. Controller design

Consider the control-oriented boiling flow oscillation system (20); the inlet flowrate, $\dot{m}_{in}$, or mass flux, G_{in}, is another manipulated variable for feedback control. In addition to nominal inlet flow, G_{in}^0, there is a feedback control law on flow change, $u = \delta G_{in}$, driven by the supply pump,

$$u = \delta G_{in} = K(x) \cdot \frac{d(\delta G)}{dt}, \quad \delta G = G - G_{in}^0 \tag{32}$$

then the normalized closed-loop flow oscillation system becomes

$$\frac{d^2(\delta G)}{dt^2} + \frac{1}{L}\left[\frac{\partial(\Delta P_c)}{\partial G} - \frac{P^2 A K(x)}{\rho_l P_0 V_0}\right]\frac{d(\delta G)}{dt} + \frac{P^2 A(\delta G)}{\rho_l P_0 V_0 L} = 0 \tag{33}$$

To maintain a stable boiling flow system, the stabilizing flow condition can be guaranteed if

$$\frac{\partial(\Delta P_c)}{\partial G} - \frac{P^2 A}{\rho_l P_0 V_0} K(x) > 0 \tag{34}$$

That is,

$$\frac{2fLG_c}{D\rho_l}g'(x) - \frac{P^2AK(x)}{\rho_l P_0 V_0} \geqslant 0 \tag{35}$$

or equivalently

$$\begin{aligned} K(x) &\leqslant \frac{2fLG_cP_0V_0}{DP^2A}\frac{a_3-1}{2a_2}[3(a_1x)^2 + 4b(a_1x) + 1] \\ b &= \frac{a_2}{a_1(a_3-1)} - 1 \end{aligned} \tag{36}$$

Since the quadratic function inside the bracket has a lower bound

$$3(a_1x)^2 + 4b(a_1x) + 1 \geqslant 1 - \frac{4}{3}b^2 \tag{37}$$

the condition always holds if

$$K := K(x) \leqslant \frac{2fLG_cP_0V_0}{DP^2A}\frac{a_3-1}{2a_2}\left(1 - \frac{4b^2}{3}\right) \tag{38}$$

5.3.2. Observer design

Note that the active control law (32) uses the flow acceleration dG/dt for feedback, which is not directly measured. Therefore, for feedback control, it is imperative to estimate this variable with a model-based method from the measurements of mass flowrate $\dot{m}$ or mass flux G. The general state estimation framework is similar to that developed in Zhang et al. (2010).

Defining the states $z_1 = G$, $z_2 = dG/dt$ and the manipulated input $u = G_{in}$, the control-oriented state space representation of the flow boiling oscillation system (20) becomes

$$\begin{cases} \dot{z}_1 = z_2 \\ \dot{z}_2 = -d \cdot z_1 - h(z_1) \cdot z_2 + d \cdot u \end{cases} \tag{39}$$

where the measured system output is $y = z_1$, and

$$h(z_1) = \frac{1}{L}\frac{\partial(\Delta P_c)}{\partial G}, \quad d = \frac{P^2A}{\rho_l P_0 V_0 L} > 0$$

To estimate the plant states of (39), an observer can be designed

$$\begin{cases} \dot{\hat{z}}_1 = \hat{z}_2 + F_1 \cdot (z_1 - \hat{z}_1) \\ \dot{\hat{z}}_2 = -d \cdot z_1 - h(z_1) \cdot \hat{z}_2 + d \cdot u + F_2 \cdot (z_1 - \hat{z}_1) \end{cases} \tag{40}$$

where $F = [F_1 F_2]^T$ are the observer gains to be determined. Let $\tilde{z}_1 = \hat{z}_1 - z_1, \tilde{z}_2 = \hat{z}_2 - z_2$, by subtracting (39) from (40), the state estimation error system can be obtained

$$\begin{aligned} &\begin{cases} \dot{\tilde{z}}_1 = -F_1 \cdot \tilde{z}_1 + \tilde{z}_2 \\ \dot{\tilde{z}}_2 = -F_2 \cdot \tilde{z}_1 - h(z_1) \cdot \tilde{z}_2 \end{cases} \\ &\dot{\tilde{z}} = \mathscr{A} \cdot \tilde{z}, \quad \mathscr{A} = \begin{bmatrix} -F_1 & 1 \\ -F_2 & -h(z_1) \end{bmatrix} \end{aligned} \tag{41}$$

The characteristic equation, $\det(\lambda I - \mathscr{A}) = 0$, of the error system (41) reads

$$\lambda^2 + [F_1 + h(z_1)]\lambda + F_1 h(z_1) + F_2 = 0 \tag{42}$$

Evidently, the observer error system is stable if and only if both the following conditions are satisfied,

$$F_1 + h(z_1) > 0 \tag{43}$$

$$F_1 h(z_1) + F_2 > 0 \tag{44}$$

The nonlinear function $h(z_1) = h(G)$ comes from the pressure-drop slope of two-phase flow characteristics (6)–(9), then

$$h(z_1) = \frac{1}{L}\frac{\partial(\Delta P_c)}{\partial x}\frac{\partial x}{\partial z_1} = \frac{2G_c}{D}\frac{f}{\rho_l}g'(x) \tag{45}$$

where the nonlinear function $g'(x)$ under complete/partial/no boiling conditions from (8) is given by

$$\begin{aligned} g'(x) &= \begin{cases} c_1x^2 + c_2x, & 0 \leqslant x < 1 \\ c_3x^2 + c_4x + c_5, & 1 \leqslant x < \frac{1}{a_1} \\ 2x, & \frac{1}{a_1} \leqslant x \end{cases} \\ c_1 &= 3\left[a_1 + \frac{a_2(a_3+1)}{2} - a_3\right], \quad c_2 = 2a_3, \\ c_3 &= \frac{3a_1^2(a_3-1)}{2a_2}, c_4 = 2\left[1 - \frac{a_1(a_3-1)}{a_2}\right], c_5 = \frac{a_3-1}{2a_2} \end{aligned} \tag{46}$$

Obviously, $g'(x)$ is a piecewise quadratic function, where it is negative within the two-phase flow exit (partial boiling) region. Thus, it has a minimum lower bound,

$$g'(x) = c_3\left(x + \frac{c_4}{2c_3}\right)^2 + c_5 - \frac{c_4^2}{4c_3} \geqslant c_5 - \frac{c_4^2}{4c_3}$$

Therefore, the above estimation error convergence conditions (43), and (44) still hold if

$$F_1 + h(z_1) = F_1 + \frac{2fG_c}{D\rho_l}g'(x) \geqslant F_1 + \frac{2fG_c}{D\rho_l}\left(c_5 - \frac{c_4^2}{4c_3}\right) > 0 \tag{47}$$

$$F_1 h(z_1) + F_2 \geqslant F_1\frac{2fG_c}{D\rho_l}g'(x) + F_2 > 0 \tag{48}$$

So it can be concluded that the real system states can be asymptotically estimated by the observer (40) if the observer gains, F, are chosen as

$$F_1 > \frac{2fG_c}{D\rho_l}\left(\frac{c_4^2}{4c_3} - c_5\right) > 0, \quad F_2 = F_1^2 \tag{49}$$

The observer gain here can be chosen to be sufficiently high to reduce the effect of state estimation error on a feedback control system (Khalil, 2002).

5.3.3. Closed-loop simulation

Once the system states are reconstructed by the observer, they can be used for advanced feedback control purposes. With this pump-driven active feedback control scheme, the flow oscillation can be successfully suppressed as observed in Fig. 20 since the controller is implemented at the 10th second. The inlet refrigerant flow, G_{in}, is no longer kept at the fixed value $G_{in} = 80\ \mathrm{kg/m^2\,s}$; instead, it changes with transient flow and heat load conditions. The phase portrait in Fig. 21 clearly shows that the closed-loop equilibrium pressure has not been elevated for each imposed heat load.

5.4. Closed-loop responses to periodic heat loads

A set of active control strategies have been developed in the above sections. It is also interesting to study the effect of periodic sine-wave heat loads on the closed-loop two-phase flow control system. First, the open-loop dynamic responses of the compressible flow system to different time-period heat loads are depicted in Fig. 22, where the period τ varies from 2 s, to 5 s, and to 10 s within the simulation time range (10–50 s) and the heat load variation amplitude $\Delta q = 500$ W. Obviously, the periodic heat load changes the original oscillatory flow patterns. It should be noted that the oscillatory flow under the nominal 1500 W heat load results in the critical heat flux condition being exceeded in Fig. 22. In contrast, Fig. 23 shows a desired scenario in which the closed-loop flow system responses with the pump-driven active controller, does not violate the CHF constraint. With the active flow instability control system, the heated channel wall temperature T_w is maintained below 85 °C under transient heat load changes as shown in Fig. 23.

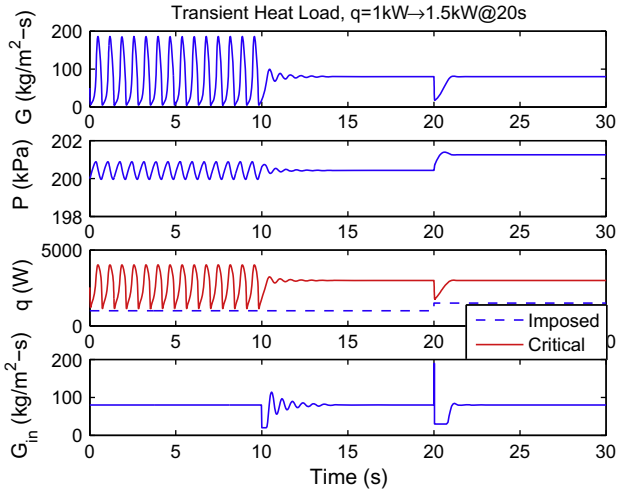

Fig. 20. Active feedback control of pressure-drop flow oscillations driven by supply pump (control implemented since the 10th second, heat load change from 1 kW to 1.5 kW since the 20th second).

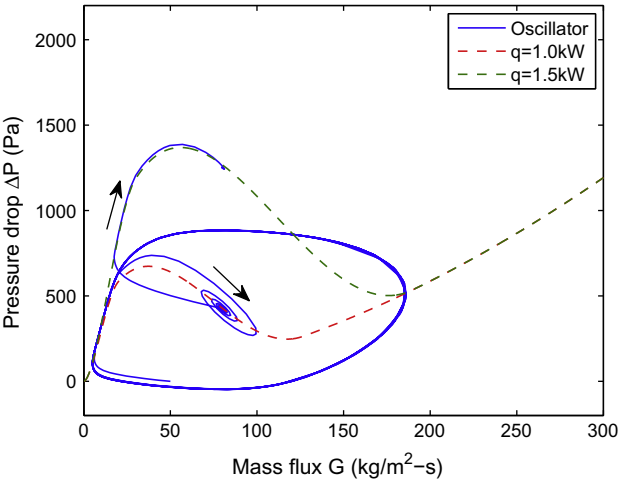

Fig. 21. Phase portrait of feedback controlled flow oscillations driven by supply pump (control implemented since the 10th second, heat load change from 1 kW to 1.5 kW since the 20th second).

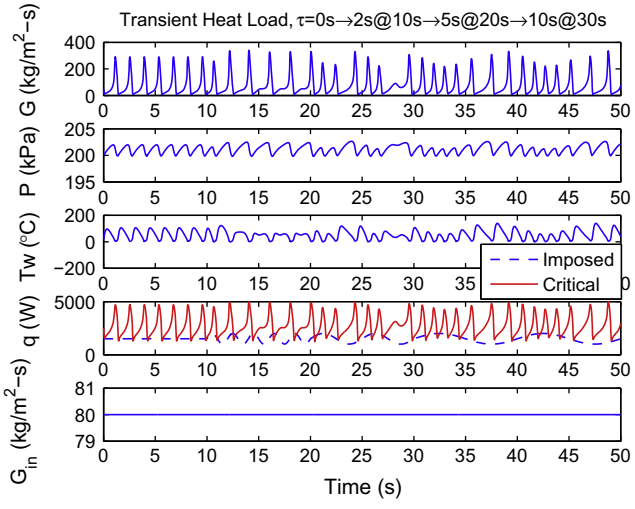

Fig. 22. Open-loop responses of pressure-drop flow/thermal oscillations to periodic heat load changes with $\tau = 2$ s, to 5 s, then to 10 s ('critical': critical heat flux times heated area).

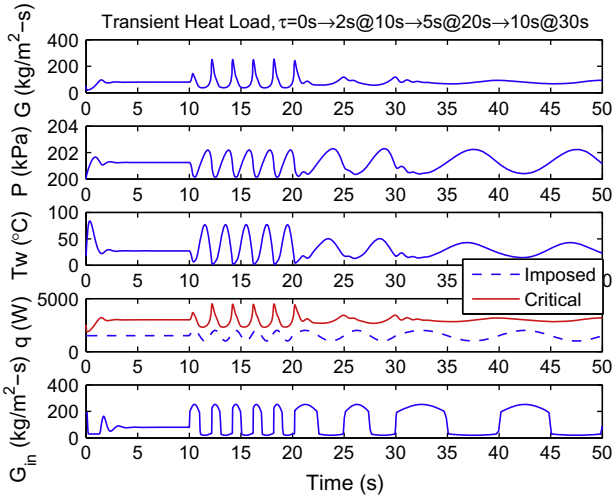

Fig. 23. Closed-loop control responses of pressure-drop flow/thermal oscillations to periodic heat load changes with $\tau = 2$ s, to 5 s, then to 10 s ('critical': critical heat flux times heated area).

6. Conclusions and discussion

Efficient and effective dynamic thermal management plays a central role in high-power electronics cooling systems. This paper is an effort to study the effects of transient heat loads on inherent flow instabilities in two-phase refrigeration cooling systems. Wall thermal inertia was shown to have strong effects on the oscillatory flow patterns since the wall thermal inertia controls the exact heat exchange rate between the external heat load and refrigerant heat absorption. Furthermore, a set of active control strategies have been developed to suppress compressible flow boiling oscillations. The steady-state CHF was employed to predict the cooling capability vs. transient heat load. Simplified two-phase friction and heat transfer correlation were used, because no widely-accepted transient two-phase heat transfer model was found in the literature. This paper has focused on one-dimensional analytical model based active two-phase flow controller design. More complicated models (i.e., three-dimensional distributed models) probably would be more capable of characterizing the two-phase system complexity, but the huge computational burden of such models hinders their usefulness for transient model predictions, and the resulting theoretical transient analysis and model-based feedback controller design would become extremely demanding. Certainly, black-box models (such as neural networks) can capture complex two-phase flow dynamics within certain operating ranges, but the prediction capability of neural network models under unspecified transient heat load changes and unstable flow conditions needs to be further studied.

In view of the issues associated with transient electronics cooling, the main control objectives are to maintain reasonable electronics wall temperatures, (that is, to guarantee the high transfer performance of two-phase flow inside the heated channel) and to avoid pressure-drop flow oscillations even under the largest transient heat load changes. For sophisticated control studies, reliable transient critical heat flux and transient two-phase heat transfer correlations are needed. Detailed experimental studies are necessary for this nascent field. In addition, the effects of wall thermal inertia on closed-loop active control system are also in need of further evaluation. Since the electronics wall (i.e., silicon die) temperatures are measurable, they can be used in advanced active electronics cooling systems in order to avoid wall burn-out in extreme cases. A natural strategy is to develop multivariable control systems, such as two feedback loops:

(1) to manipulate inlet valve to suppress the flow oscillations,
(2) to control supply pump to maintain electronics temperature,

Coordinated control policy is desired to optimize the overall transient cooling performance with low valve pressure loss and low coolant mass flowrate.

Acknowledgments

This work is supported in part by the Office of Naval Research (ONR) under the Multidisciplinary University Research Initiative (MURI) Award N00014-07-1-0723 entitled "System-Level Approach for Multi-Phase, Nanotechnology Enhanced Cooling of High-Power Microelectronic Systems," and in part by the Center for Automation Technologies and Systems (CATS) under a block grant from the New York State Foundation for Science, Technology and Innovation (NYSTAR).

Appendix A. Dynamic flow stability analysis – Lyapunov method

This appendix provides some simplified stability analysis for the compressible boiling flow system (14) and (15) by resorting to the Lyapunov stability theory.

The boiling flow oscillation model (14) and (15) is expressed as follows:

$$\frac{dG}{dt} = \frac{1}{L}(P - P_e - \Delta P_D) \tag{50}$$

$$\frac{dP}{dt} = \frac{P^2 A}{\rho_l P_0 V_0}(G_{in} - G) \tag{51}$$

Notice that the inlet mass flux, G_{in}, is actually a manipulated input for this system, $G_{in} = G_{in}^0 + u$, where u is the inlet flow variation driven by supply pump speed change. In this analysis, only the autonomous flow system is considered, that is, $u = 0$. Then defining $\delta G = G - G_{in}$, $\delta P = P - P_0$ where G_{in}^0 and P_0 are the initial equilibrium of inlet mass flux and pressure, the normalized flow model becomes

$$\frac{d(\delta G)}{dt} = \frac{1}{L}(\delta P + P_0 - P_e - \Delta P_D) \tag{52}$$

$$\frac{d(\delta P)}{dt} = -C_s \cdot \delta G, \quad C_s = \frac{P^2 A}{\rho_l P_0 V_0} \tag{53}$$

where $C_s > 0$ is approximated to be constant since $\delta P/P_0 \leqslant 1\%$ in this study or as in (Zhang et al., 2010). The demand pressure drop is a nonlinear function of mass flux that can be approximated by,

$$\Delta P_D = \Delta P_D^0 + \frac{\partial(\Delta P_D)}{\partial G}\delta G \tag{54}$$

At the initial system equilibrium, one has

$$P_0 - P_e - \Delta P_D^0 = 0 \tag{55}$$

A positive-definite Lyapunov function V is defined for the normalized flow system (52) and (53),

$$V = \frac{1}{2}C_s L(\delta G)^2 + \frac{1}{2}(\delta P)^2 \tag{56}$$

then its time derivative becomes

$$\begin{aligned}\frac{dV}{dt} &= C_s L(\delta G)\frac{d(\delta G)}{dt} + (\delta P)\frac{d(\delta P)}{dt} \\ &= C_s(\delta G)\left[\delta P - \frac{\partial(\Delta P_D)}{\partial G}(\delta G)\right] + (\delta P)[-C_s(\delta G)]\end{aligned} \tag{57}$$

where the second equality is from Eqs. (54) and (55). The derivative of the Lyapunov function is

$$\frac{dV}{dt} = -C_s(\delta G)^2\frac{\partial(\Delta P_D)}{\partial G} \tag{58}$$

where $C_s(\delta G)^2$ is always positive. Therefore, if the two-phase flow pressure-drop slope is positive,

$$\frac{\partial(\Delta P_D)}{\partial G} > 0 \tag{59}$$

the original compressible flow system (14) and (15) is proved to be asymptotically stable with the well-known Lyapunov stability theorem (Khalil, 2002).

Remark. Although the stability analysis is limited to the compressible flow system rather than the comprehensive thermal-fluid dynamics (17)–(19), the above analysis can be extended since the slow wall temperature dynamics (19) are usually stable with the exclusion of the fast flow dynamics (14) and (15) or (17) and (18).

References

Astrom, K.J., Bell, R.D., 2000. Drum-boiler dynamics. Automatica 36, 363–378.
Beitelmal, M.H., Patel, C.D., 2006. Model-based approach for optimizing a data center centralized cooling system. Hewlett-Packard (HP) Lab Technical Report.
Bergles, A.E., Lienhard, J.H., Kendall, G.E., Griffith, P., 2003. Boiling and evaporation in small diameter channels. Heat Transfer Eng. 24, 18–40.
Carey, V.P., 2008. Liquid–Vapor Phase-Change Phenomena: An Introduction to the Thermophysics of Vaporization and Condensation Processes in Heat Transfer Equipment, second ed. Taylor & Francis, New York.
Catano, J., Zhang, T.J., Zhou, R.L., Jensen, M.K., et al., 2010. Experimental identification of evaporator dynamics for vapor compression refrigeration cycle during phase transition. In: Proceedings of ITherm, June 2010, Las Vegas, Nevada.
Chang, J.Y., Park, H.S., Jo, J.I., Julia, S., 2006. A system design of liquid cooling computer based on the micro cooling technology. In: Proceedings of ITherm 2006, San Diego, CA, pp. 157–160.
Eborn, J., 2001. On model libraries for thermo-hydraulic applications. Ph.D. Thesis. Department of Automatic Control, Lund Institute of Technology, Sweden.
Garimella, S.V., Fleischer, A.S., Murthy, J.Y., et al., 2008. Thermal challenges in next-generation electronic systems. IEEE Trans. Compon. Pack. Technol. 31, 801–815.
Gilmore, D.G. (Ed.), 2002. Spacecraft Thermal Control Handbook, second ed. American Institute of Aeronautics and Astronautics Press.
Kakac, S., Bon, B., 2008. A review of two-phase flow dynamic instabilities in tube boiling system. Int. J. Heat Mass Transfer 51, 399–433.
Kakac, S., Cao, L., 2009. Analysis of convective two-phase flow instabilities in vertical and horizontal in-tube boiling systems. Int. J. Heat Mass Transfer 52, 3984–3993.
Kandlikar, S.G., 1990. A general correlation for two-phase flow boiling heat transfer inside horizontal and vertical tubes. ASME J. Heat Transfer 112, 219–228.
Kandlikar, S.G., Bapat, A.V., 2007. Evaluation of jet impingement, spray and microchannel chip cooling options for high heat flux removal. Heat Transfer Eng. 28, 911–923.
Kandlikar, S.G., Garimella, S., Li, D., et al., 2006. Heat Transfer and Fluid Flow in Minichannels and Microchannels. Elsevier.
Katto, Y., 1978. A generalized correlation of critical heat flux for the forced convective boiling in vertical uniformed heated round tubes. Int. J. Heat Mass Transfer 21, 1527–1542.
Khalil, H.K., 2002. Nonlinear Systems. third ed. Prentice Hall, Upper Saddle River, NJ.
Kuo, C.-J., Peles, Y., 2009. Pressure effects on flow boiling instabilities in parallel microchannels. Int. J. Heat Mass Transfer 52, 271–280.
Lee, J., Mudawar, I., 2009. Low-temperature two-phase microchannel cooling for high-heat-flux thermal management of defense electronics. IEEE Trans. Compon. Pack. Technol. 32, 453–465.
Lee, H.J., Yao, S.-C., 2010. System instability of evaporative micro-channels. Int. J. Heat Mass Transfer 53, 1731–1739.
Liu, H.T., Kocak, H., Kakac, S., 1995. Dynamical analysis of pressure-drop type oscillations with a planar model. Int. J. Multiphase Flow 21, 851–859.
Ozawa, M., Akagawa, K., Sakaguchi, T., Tsukahara, T., Fujii, T., 1979. Flow instabilities in boiling channels – Part 1. Pressure-drop oscillation. Bull. JSME 22, 1113–1118.
Schmidt, R.R., Notohardjono, B.D., 2002. High-end server low-temperature cooling. IBM J. Res. Dev. 46, 739–751.
Thome, J.R., 2006. State-of-the-art overview of boiling and two-phase flows in microchannels. Heat Transfer Eng. 27, 4–19.
Trutassanawin, S., Groll, E.A., Garimella, S.V., Cremaschi, L., 2006. Experimental investigation of a miniature-scale refrigeration system for electronics cooling. IEEE Trans. Compon. Pack. Technol. 29, 678–687.
Wadell, R., Joshi, Y.K., Fedorov, A.G., 2007. Experimental investigation of compact evaporators for ultralow temperature refrigeration of microprocessors. ASME J. Electron. Pack. 129, 291–299.
Wang, K., Eisele, M., Hwang, Y., Radermacher, R., 2010. Review of secondary loop refrigeration systems. Int. J. Refrig. 32, 212–234.

Webb, T.W., Kiehne, T.M., Haag, S.T., 2007. System-level thermal management of pulsed loads on an all-electric ship. IEEE Trans. Magn. 43, 469–473.
Xu, J., Zhou, J., Gan, Y., 2005. Static and dynamic flow instability of a parallel microchannel heat sink at high heat fluxes. Energy Convers. Manage. 46, 313–334.
Xu, J., Liu, G., Zhang, W., Li, Q., Wang, B., 2009. Seed bubbles stabilize flow and heat transfer in parallel microchannels. Int. J. Multiphase Flow 35, 773–790.
Yin, J., 2004. Modeling and analysis of multiphase flow instabilities. Ph.D. Thesis. Rensselaer Polytechnic Institute.
Zhang, T.J., Tong, T., Peles, Y., Prasher, R., et al., 2009. Ledinegg instability in microchannels. Int. J. Heat Mass Transfer 52, 5661–5674.
Zhang, T.J., Peles, Y., Wen, J.T., et al., 2010. Analysis and active control of pressure-drop flow instabilities in boiling microchannel systems. Int. J. Heat Mass Transfer 53, 2347–2360.
Zhou, R.L., Catano, J., Zhang, T.J., Wen, J.T., et al., 2009. The steady-state modeling and analysis of a two-loop cooling system for high heat flux removal. In: Proceedings of 2009 ASME-IMECE, Orlando, FL.